

Temperature dependence of ferroelectric and dielectric properties of textured $0.98(0.94\text{Na}_{0.5}\text{Bi}_{0.5}\text{TiO}_3-0.06\text{BaTiO}_3)-0.02\text{K}_{0.5}\text{Na}_{0.5}\text{NbO}_3$ thick film

Fang Fu · Jiwei Zhai · Zhengkui Xu ·
Chenggen Ye · Xi Yao

Received: 13 June 2010/Accepted: 25 August 2010/Published online: 8 September 2010
© Springer Science+Business Media, LLC 2010

Abstract Textured $0.98(0.94\text{Na}_{0.5}\text{Bi}_{0.5}\text{TiO}_3-0.06\text{BaTiO}_3)-0.02\text{K}_{0.5}\text{Na}_{0.5}\text{NbO}_3$ thick film was prepared by reactive templated grain growth (RTGG) method. The effect of temperature on ferroelectric and dielectric behaviors of the thick film was investigated. Its dielectric constant as a function of temperature displayed typical relaxation behavior, which was similar to that of NBT-based bulk ceramics. Remnant polarization, saturation polarization, and coercive field of the thick film all decreased with increasing temperature. Dielectric constant and tunability of the film were also dependent on temperature. Electric field dependence of dielectric constant of the thick film suggested a transition from ferroelectric to antiferroelectric phase at around the depolarization temperature. A strong increase in leakage current density with increasing temperature was observed, which could be related to the enhanced activity of conductivity carriers.

Introduction

Piezoelectric thick films draw significant interest in recent years for their applications in micro-electro-mechanical system (MEMS). They are widely applied to micropumps, ultrasonic motors, resonators, high-frequency transducers, and energy harvestors [1–3]. Thick films on low-cost substrates could be more suitable for commercial applications

because they do not have the problems of large dielectric loss observed in thin films and high voltages required by bulk materials. Lead-containing materials are currently dominating the market of piezoelectric thick films. However, lead-containing materials are toxic and thus not environmental friendly. As a result, there has been a strong tendency to develop lead free materials because of the demands for environmental protection [4–7]. Zhang et al. [8] fabricated lead free piezoelectric ceramics with a composition of $0.92\text{NBT}-0.06\text{BT}-0.02\text{KNN}$ which possessed very promising d_{33} . However, information on piezoelectric properties of lead free thick films is rarely available. Zhang and Jiang [9] used screen-printing processing and infiltration route to fabricate $\text{Bi}_{0.5}(\text{Na}_{0.82}\text{K}_{0.18})_{0.5}\text{TiO}_3$ lead free thick film, which had a longitudinal effective piezoelectric coefficient $d_{33\text{eff}}$ of 109 pm/V. This value cannot catch up with that of PZT thick films ($d_{33} = 210$ pm/V [10]). Recently, we found that $0.98(0.94\text{NBT}-0.06\text{BT})-0.02\text{KNN}$ (NBT–BT–KNN2) textured thick film had improved piezoelectric constant. d_{33} value of the NBT–BT–KNN2 textured thick film with 75% grain orientation was 349 pm/V.

However, little is known about temperature stability of the thick film which is often desirable for practical applications. Electric devices may need to work at different temperatures, so it is necessary to evaluate electric behavior of the materials as a function of temperature. It was reported that the potential well at ferroelectric domain boundaries becomes more box-like shaped with decreasing temperature, where more charged defects can migrate to and be trapped. The trapped defects play a great role in determining domain switching. Therefore, macroscopic ferroelectric responses, such as P_r , P_s , and E_c , are varied with temperature accordingly [11–15].

In the present study, we investigated temperature dependences of dielectric constant and loss tangent of a

F. Fu · J. Zhai (✉) · C. Ye · X. Yao
Functional Materials Research Laboratory, Tongji University,
Shanghai 200092, China
e-mail: apzhai@tongji.edu.cn

Z. Xu
Department of Physics and Materials Science,
City University of Hong Kong, Kowloon, Hong Kong

NBT–BT–KNN2 textured thick film. The variation in P_r , P_s , and E_c of the material will be discussed in detail. Dielectric constant as a function of electric field at different temperatures was measured. Temperature dependence of leakage current density of the film was also studied.

Experimental

0.98(0.94NBT–0.06BT)–0.02KNN (NBT–BT–KNN2) textured thick film was fabricated by tape-casting method. The NBT powders were synthesized via a solid state route with analytical reagent Bi_2O_3 , NaCO_3 , and TiO_2 powders as raw materials. The mixture of raw materials was ball milled in dehydrated alcohol for 24 h and then calcined at 880 °C for 2 h. The KNN powders were also prepared by solid state reaction method. BT powder was supplied by Guoteng Functional Materials Limited Company in Shandong province, China. The matrix with a composition of 0.98(0.94NBT–0.06BT)–0.02KNN was prepared with NBT, KNN, and BT powders. Plate-like $\text{Bi}_4\text{Ti}_3\text{O}_{12}$ particles were used as templates. They were synthesized from Bi_2O_3 and TiO_2 via a salt molten method. The mixture of 80 wt% matrix and 20 wt% $\text{Bi}_4\text{Ti}_3\text{O}_{12}$ templates was ball milled in solvent for 15 h. An organic bonding (LS model, produced by Lingguang Electric Chemical Materials Technology Corporation in Zhaoqing city, China) was added to stabilize the suspension. The stable slurry was tape cast with a conventional tape-casting equipment. The

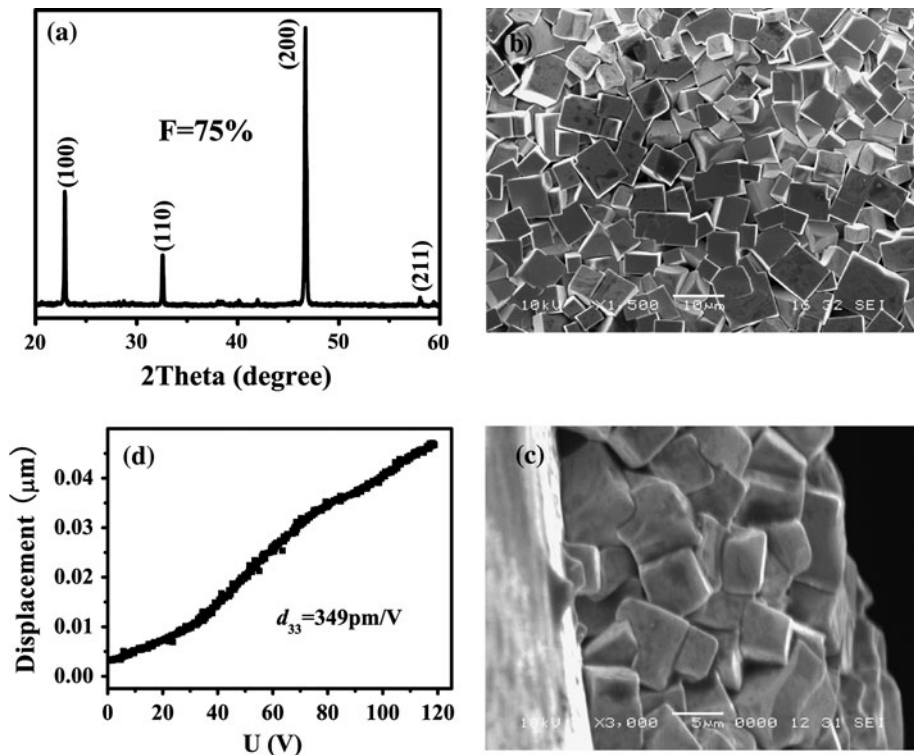
dried green film was cut and pressed on platinum substrate by isostatic pressing at 200 MPa. The sample was annealed at 550 °C to remove the organic substance and then sintered at 1,250 °C for 2 h.

Gold electrode with a thickness of 80 nm and a diameter of 0.5 mm was coated on surface of the thick film for electric characterization. Temperature dependence of dielectric constant and loss tangent of the sample were measured from 50 to 350 °C at different frequencies using a high-precision LCR meter (HP 4284A). P – E hysteresis loops of the thick film were measured at different temperatures by using a ferroelectric test system (Precision PremierII, made in USA). Tunability was measured up to 100 kV/cm by using a Keithley model 2410 electrometer coupled with a TH2613A LCR meter. Leakage current density of the thick film was tested with a Keithley 6517A Electrometer (Cleveland, OH).

Results and discussion

Figure 1a shows XRD patterns of the NBT–BT–KNN2 thick film. The thick film possesses perovskite structure. Its grain orientation degree is characterized by Lotgering's factor [16] which reaches to 75%. SEM image of the film is shown in Fig. 1b. The sample has approximately 6 μm cubic grains. Thickness of the thick film is about 20 μm as shown in Fig. 1c. Figure 1d shows unipolar electric field-induced strain curves of the NBT–BT–KNN2 thick film.

Fig. 1 XRD pattern (a), surface morphology (b), cross-section image (c), and unipolar electric field-induced strain curve (d) of the NBT–BT–KNN2 thick film



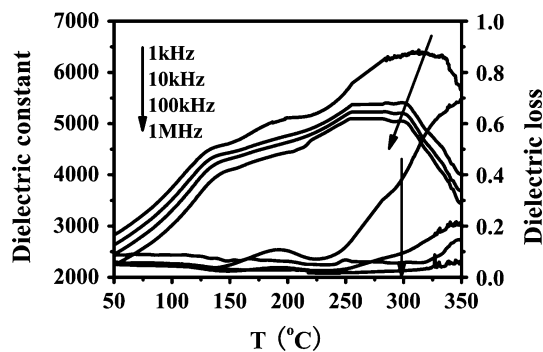


Fig. 2 Temperature dependence of dielectric constant and loss tangent of the NBT–BT–KNN2 thick film

Piezoelectric constant d_{33} can be calculated by the formula $d_{33} = S_{\max}/E_{\max}$, where S_{\max} and E_{\max} represent the maximum values of strain and electric field. The value of d_{33} reaches to 349 pm/V which is higher than that of PZT–thick film.

Figure 2 shows temperature dependence of dielectric constant (ε) and loss tangent ($\tan \delta$) of the NBT–BT–KNN2 thick film at 1, 10, 100, and 1,000 kHz. Two abnormal dielectric peaks are observed over 50–350 °C. The temperature of the first peak is called depolarization temperature (T_d), which corresponds to the phase transition from ferroelectric to antiferroelectric. The temperature corresponding to the maximum value of dielectric constant is Curie temperature (T_m). The frequency dependence and dispersion indicate typical relaxor behavior of the thick film. The dielectric constant decreases with increasing frequency in a way similar to that observed in relaxed-like materials, such as $(\text{Bi}_{0.5}\text{Na}_{0.5})\text{TiO}_3$ – $(\text{Bi}_{0.5}\text{K}_{0.5})\text{TiO}_3$ and $[\text{Bi}_{0.5}(\text{Na}_{1-x-y}\text{K}_x\text{Li}_y)_{0.5}]\text{TiO}_3$ [17, 18].

A modified empirical expression Curie–Weiss law proposed by Uchino and Nomura [19] was used to quantify the diffuseness of a phase transition:

$$\frac{1}{\varepsilon_r} - \frac{1}{\varepsilon_m} = \frac{(T - T_m)^\alpha}{C},$$

where ε_r and ε_m are the dielectric constant at temperature T and the maximum permittivity at Curie temperature T_m , respectively. The parameter α is called diffusion exponent ranging from 1 to 2. The value of α can be obtained from slope of linear relationship between $\ln(1/\varepsilon_r - 1/\varepsilon_m)$ and $\ln(T - T_m)$ as shown in Fig. 3. The diffusion exponent α increases with increasing frequency. This behavior is significant for a relaxation process and could be ascribed to the compositional fluctuation or structural disordering of the thick film. The loss tangent increases rapidly as a result of the strong conductivity at high temperature.

Figure 4a–c shows P – E hysteresis loops of the NBT–BT–KNN2 textured thick film at different temperatures.

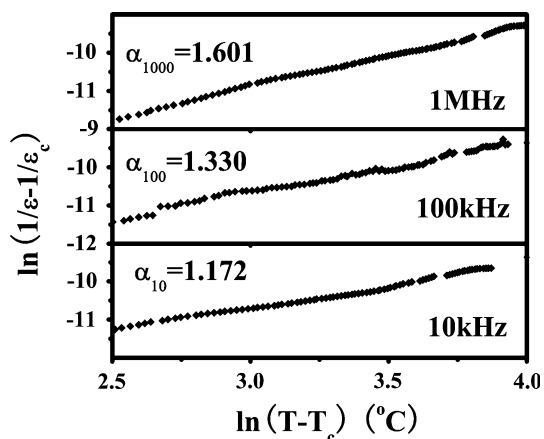


Fig. 3 $\ln(1/\varepsilon_r - 1/\varepsilon_m)$ as a function of $\ln(T - T_m)$ of the NBT–BT–KNN2 thick film

The P – E loop at room temperature exhibits typical ferroelectric characterization. The loops become slimmer together with the reduction of P_r and E_c with increasing temperature. The pinched shape of the P – E loops above 70 °C indicates the transition from a ferroelectric phase to an antiferroelectric one. Afterward, the P – E loops are deformed, having a strong asymmetry at temperature above 150 °C. Hagh et al. [20] suggested that the area enclosed by a hysteresis loop corresponds to the amount of energy dissipated in the form of heat. This result indicated that the deformed P – E loops of the thick film should be attributed to its strong loss tangent at high temperature. The transformation of P – E loops from a ferroelectric to an antiferroelectric one is the result of the electromechanical interaction between the ferroelectric and antiferroelectric regions that coexisted in the thick film at high temperatures, according to Lin et al. [4]. The depolarization temperature of the thick film determined from P – E loops suggests a range approximately from 110 to 130 °C, which also confirmed the coexistence of ferroelectric phase and antiferroelectric phase.

P_r is determined by the spontaneously polarized domains which are unswitchable at an applied electric field, whereas the P_s is determined by the total polarized domains including switchable ones. In general, the volume of switchable domains V_{switch} is related to the value of $P_s - P_r$. Temperature dependence of $P_s - P_r$ is plotted in Fig. 5. We selected the temperature range of 15–50 °C which is below the phase transition temperature. V_{switch} shows a tendency of reduction with increasing temperature. $P_s - P_r$ versus temperature is plotted in Fig. 5. The Arrhenius law is defined as

$$P_s - P_r = P_0 \exp(-E/k_B T),$$

where E is the average activation energy of switchable domains, k_B is the Boltzmann's constant, and P_0 is a

Fig. 4 P - E hysteresis loops of the NBT-BT-KNN2 thick film at different temperatures
(a) 15–50 °C, **(b)** 70–130 °C,
(c) 150–190 °C, **(d)** remnant polarization and the coercive field as a function of temperature

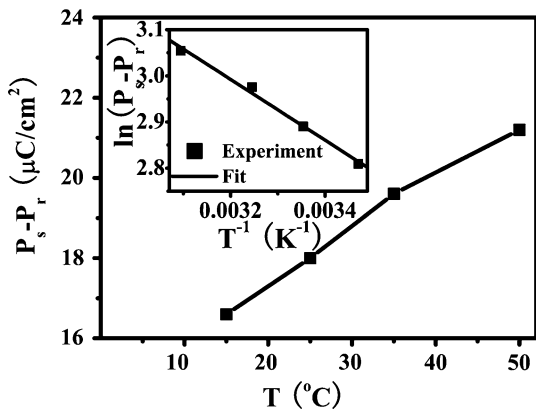
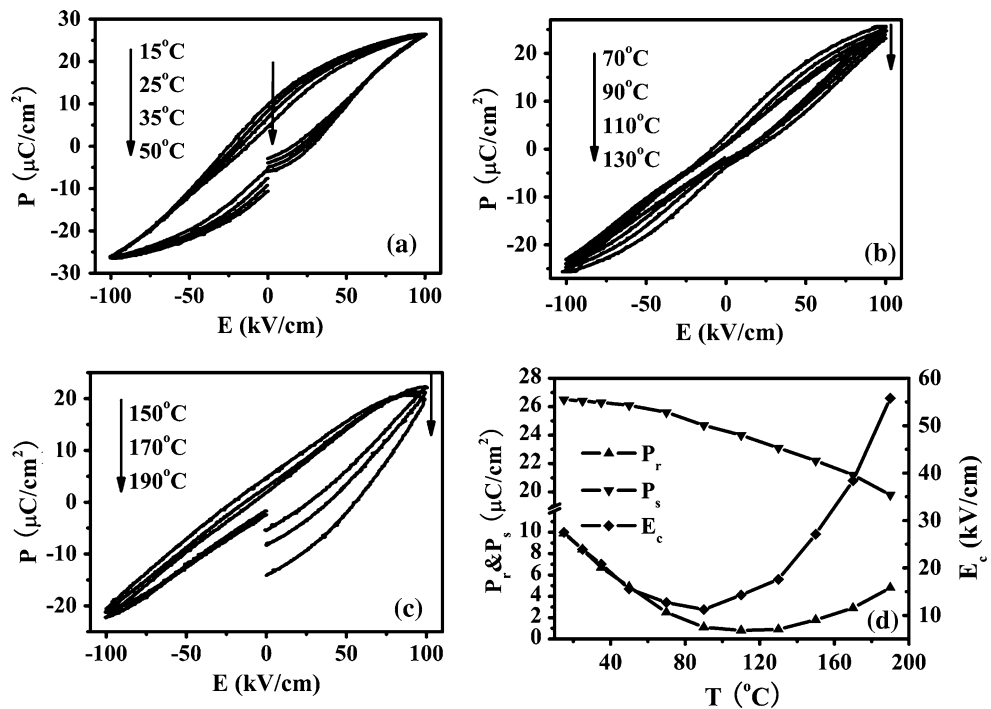


Fig. 5 Relationship between $P_s - P_r$ and temperature of the NBT-BT-KNN2 thick film

constant. The relationship of $P_s - P_r$ and temperature obeys the Arrhenius law. The slope of $\ln(P_s - P_r) - 1/T$ can be used to estimate the average activation energy of domain switching.

Dielectric constants as a function of electric field measured at different temperature are shown in Fig. 6a, b. The strong domain pinning at lower temperature depressed the contribution of the domain wall motion to dielectric constant and consequently reduced the dielectric constant. Furthermore, the tunability (defined as $(\epsilon_{\max} - \epsilon_{\min})/\epsilon_{\max}$), which indicates the ferroelectric domain switching contribution to dielectric constant, decreases with decreasing temperature. It is reasonable because the number of switchable domains is decreased at low temperature [21].

The relationship between dielectric constant and electric field at different temperatures qualitatively indicates a temperature-dependent domain switching behavior of the thick film. The ϵ - E curves deformed at temperatures above 130 °C, which suggest the phase transition from a ferroelectric phase to an antiferroelectric one.

Figure 7 shows relationship between leakage current density and applied electric field at different temperatures. The leakage current density increases with increasing temperature. The value at 50 kV/cm increases from $1.4 \times 10^{-5} \text{ A}/\text{cm}^2$ at 40 °C to $2.1 \times 10^{-5} \text{ A}/\text{cm}^2$ at 100 °C and reaches to $3.8 \times 10^{-5} \text{ A}/\text{cm}^2$ at 150 °C. Thermal energy generated at high temperature is provided for exciting the carriers, making them jump out from ground state and freely move in the material. The increase in the number of free carriers results in the large leakage current density. As a result, the conductivity at high temperature strongly improves, which is also responsible for the large loss tangent and the distortion of P - E loops at high temperatures in Figs. 2, 4c.

Conclusions

Dielectric and ferroelectric properties of a NBT-BT-KNN2 thick film as a function of temperature were investigated. Its temperature dependence of dielectric constant and loss tangent had relaxor characteristics. The diffusion exponent α increased with increasing frequency. P_r , P_s , and E_c all decreased with increasing temperature

Fig. 6 Electric field dependence of dielectric constant of the NBT–BT–KNN2 thick film at different temperatures (a) 15–90 °C and (b) 110–150 °C

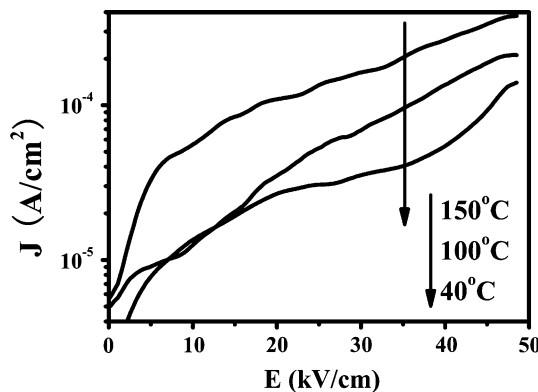
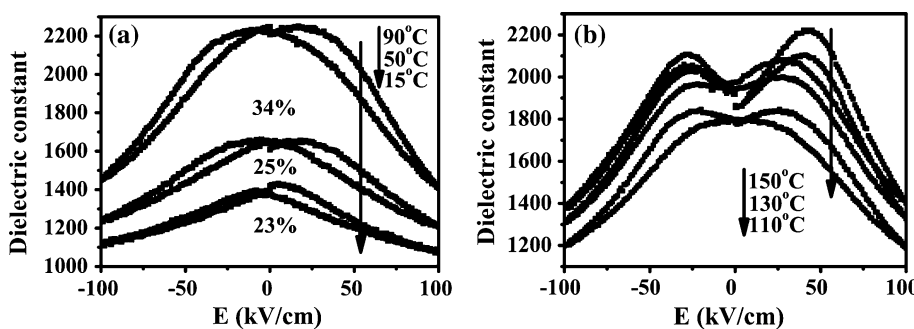


Fig. 7 Relationship between leakage current density and applied electric field at different temperatures

below T_d . The pinched sharp of the $P-E$ loops at around the depolarization temperature indicated the transition from a ferroelectric phase to an antiferroelectric one. The $P-E$ loops further deformed above depolarization temperature because of the strong leakage current density. Tunability increased with increasing temperature. Leakage current density also had a tendency of increase with increasing temperature because of the enhanced activity of the free carriers.

Acknowledgements The authors would like to acknowledge the support from the National Natural Science Foundation of China under grant No. 50972108, 50932007 and Shanghai Foundation Project under grant 08JC1419100. It was also partially supported by the Research Grants Council of the Hong Kong Special Administrative Region, China (CityU No. 103307).

References

1. Pu Z, Wu J, Yu X, Xu P, Cheng L, Xiao D, Zhu J (2008) Surf Coat Technol 202:2068
2. Ursic H, Hrovat M, Belavic D, Cilensek J, Drnovsek S, Holc J, Zarnik M, Kosec M (2008) J Eur Ceram Soc 28:1839
3. Kuscer D, Skalar M, Holc J, Kosec M (2009) J Eur Ceram Soc 29:105
4. Lin D, Kwok KW, Chan HLW (2008) Solid State Ionics 178:1930
5. Zuo R, Ye C, Fang X, Li J (2008) J Eur Ceram Soc 28:871
6. Takenaka T, Maruyama K, Sakata K (1991) Jpn J Appl Phys 30:2236
7. Nagata H, Takenaka T (1997) Jpn J Appl Phys Part 1 36:6055
8. Zhang S, Koung AB, Aulbach E, Ehrenberg H, Rödel J (2007) Appl Phys Lett 91:112906
9. Zhang H, Jiang S (2009) J Eur Ceram Soc 29:717
10. Osone S, Brinkman K, Shimojo Y, Iijima T (2008) Thin Solid Films 516:4325
11. Dimos D, Al-Shareef HN, Warren WL, Tuttule BA (1996) J Appl Phys 80:1682
12. Dawber M, Scott JF (2000) Appl Phys Lett 76:1060
13. Noguchi Y, Miyayama M (2001) Appl Phys Lett 78:1903
14. Desu SB (1995) Phys Status Solidif A 151:467
15. Brennan C (1993) Ferroelectrics 150:199
16. Fujimura N, Nishihara T, Goto S, Xu J, Ito T (1993) J Cryst Growth 130:269
17. Sasaki A, Chiba T, Mamiya Y, Otsuki E (1999) Jpn J Appl Phys 38:5564
18. Lin D, Xiao D, Zhu J, Yu P (2006) Appl Phys Lett 88:062901
19. Uchino K, Nomura S (1982) Ferroelectric Lett Sect 44:55
20. Hagh NM, Kerman K, Jadidian B, Safari A (2009) J Am Ceram Soc 29:2325
21. Zhang S, Chen Z, Zhang C, Yuan G (2010) Appl Surf Sci 256:2468